Journal of Applied Polymer Science

Nanostructured Membrane Electrode Assemblies from Layer-by-Layer Composite/Catalyst Containing Membranes and Their Fuel Cell Performances

Hüseyin Deligöz, Serpil Yılmaztürk, Tolga Gümüşoğlu
Engineering Faculty, Chemical Engineering Department, Istanbul University, 34320 Avcilar-Istanbul, Turkey
Correspondence to: H. Deligöz (E-mail: hdeligoz@istanbul.edu.tr)

ABSTRACT: In this study, two approaches are compared to develop nanostructured membrane electrode assemblies (MEA) using layer-by-layer (lbl) technique. The first is based on the direct deposition of polyallylamine hydrochloride (PAH) and sulfonated polyaniline (sPAni) on Nafion support to prepare lbl composite membrane. In the second approach, sPAni is coated on the support in the presence of platinum (Pt) salt, Nafion solution and Vulcan for obtaining catalyst containing membranes (CCMs). SEM and UV–vis analysis show that the multilayers are deposited on both sides of Nafion successfully. Although H_2/O_2 single cell performances of acid doped lbl composite membrane based MEA are found to be at the range of 126 and 160 mW cm^{-2} depending on the number of deposited layers, the cell performance of MEA obtained from catalyst containing lbl self-assembled thin membrane $(PAH/sPAni\text{-}H^+)_{10\text{-}Pt}$ is found to be 360 mW cm^{-2} with a Pt utilization of 720 mW $mgPt^{-1}$. This performance is 82% higher as compared to original Nafion®117 based MEA (198 mW cm^{-2}). From the cell performance evaluations for different structured MEAs, it is mainly found out that the use of lbl CCMs instead of composite membranes and fabrication of thinner electrolytes result in a higher H_2/O_2 cell activity due to significant reduction in ohmic resistivity. Also, it is observed that the use of sPAni slightly improves the cell performance due to an increased probability of the triple phase contact and it can lead to superior physicochemical properties such as conductivity and thermal stability. © 2014 Wiley Periodicals, Inc. J. Appl. Polym. Sci. **2014**, *131*, 40314.

KEYWORDS: batteries and fuel cells; membranes; self-assembly; catalysts

Received 17 October 2013; accepted 17 December 2013
DOI: 10.1002/app.40314

INTRODUCTION

A single proton exchange membrane fuel cell (PEMFC) mainly consists of three types of components: a membrane electrode assembly (MEA), a bipolar plate (BPP) and a seal.[1] Among these components, the key part of a fuel cell is the MEA, where the electrochemical reactions occur and electricity is produced. The fabrication of MEAs with higher fuel cell performance has a paramount importance. Nowadays, many techniques have been exploited to fabricate MEAs, in which, the electro catalyst could be coated either onto a gas diffusion layer or directly onto an electrolyte membrane.[2,3] In the last decade, the preparation of catalyst containing membrane (CCM) has attracted more attention for achieving higher performance and lower cost. In this technique, the catalyst layers are directly applied to both sides of the electrolyte and it is believed that the MEA prepared by CCM technique yields higher cell performance than the gas diffusion layer (GDL) based MEA due to higher catalyst utilization[4,5] and a better electrolyte/catalyst interface.[5–7] There are several different methods for the preparation of catalyst containing membranes such as spraying,[8–15] painting,[16] decaling technique,[17–20] screen, and inkjet printing.[21,22]

Layer-by-layer (lbl) technique was firstly reported by Decher as a promising and efficient method for the preparation of multilayered ultrathin films in a simple way.[23] A major advantage gained from lbl technique in fuel cell (FC) applications is the introduction of a large number of variables that modify the properties of electrolytes and electrodes depending on the experimental conditions. Other advantages of lbl method are the use of low cost, nontoxic polyelectrolyte materials, simple fabrication process, and miniaturization of the electrochemical components.[24]

In the last years, electrically conducting polymers described as a new class of "synthetic metals" attracted increasing attention. Polyaniline (PAni) exhibits lots of outstanding properties such as tunable conductivity from insulator to metal, oxidative, and environmental stability depending on its oxidation state and pH.[25,26] PAni can be prepared by both chemical[26–28] and electrochemical methods. The combination of versatile properties of

PAni makes it useful for various applications including rechargeable batteries,[29] light emitting diodes[30] and electrochromic displays.[31] On the other hand, synthesis of sulfonated PAni (sPAni), which is known as self-doping polymer, and first water soluble conducting derivatives of PAni was reported in the beginning of 1990s by Yu and Epstein[32] and McDiarmid et al.[33]

In the last a few years, lbl multilayered membranes with high proton conductivity and reduced methanol diffusivity were reported for fuel cell applications.[34–38] Furthermore, some groups attempted to prepare lbl polyelectrolyte-carbon electrode (LPCE) MEAs for H_2/O_2 fuel cell systems.[24,39–45] Farhat and Hammond reported that lbl polymer-carbon electrodes can be considered as an important alternative to conventional graphitic slurry and carbon cloth type electrodes. They claimed that LPCEs prepared from PDAC [poly(diallyl dimethylammonium chloride)] and PAMPSA [poly(2-acrylamido-2-methyl-1-propanesulfonic acid)]/Hispec3000 were capable of withstanding strong acidic, basic, or oxidizing media. In that study, open-circuit potential (OCP) and maximum power density of self-assembled PDAC/PAMPS MEA performing under H_2/air were found to be almost +0.9 V and 2.0 mW cm^{-2}, respectively.[41] In another study, Michel et al. have recently demonstrated that fuel cells with lbl catalyst layers comprising single walled carbon nanotubes (SWCNTs) and carbon fibers (CFs) exhibited peak power densities of 195 and 227 mW cm^{-2}, respectively.[24] In another study of this group, highly active, carbon supported Pt electrocatalysts were synthesized using a supercritical fluid method and a selective heterogeneous nucleation reaction to disperse Pt on SWCNT and CF supports. Finally, it was found much higher Pt utilizations, 3198 mW $mgPt^{-1}$ than that of MEA produced using conventional methods (~800 mW $mgPt^{-1}$).[44] Very recently, our group reported the preparation of CCMs using four different lbl fabrication techniques and it was found that the use of anionic polyelectrolyte, platinum salt, Nafion solution, and carbon mixture resulted in higher PEM cell power output.[46] In a different work reported by Michel et al., it was demonstrated that the incorporation of functionalized polyaniline fibers (Pt/PAni-F) in lbl structures can give high fuel cell performance and Pt utilization due to the high conductance of PAni-F as well as ion/gas transport.[47]

As it is known, fuel cell electrodes require three essential properties: They should be electronically conductive, proton conductive, and able to trigger a chemical reaction catalyzed by a metal.[46,47] Since sPAni is water soluble and has parallel electronic/ionic conductivity, it is possible to create nano-thickness conductive multilayers with an increased probability of the triple-phase contact using lbl technique. In this contribution, two approaches are studied to develop nanostructured membrane electrode assemblies (MEA) based on lbl self-assembled composite and catalyst containing membranes from PAH and sPAni. In the first part of the study, preparation, and characterization of both self-assembled composite and catalyst containing membranes are reported. In the second part, single cell performances of lbl composite and catalyst containing membrane based MEAs are compared in conjunction with the use of conductive sPAni and the thickness of membrane support. Also, the influences of acid treatment and thickness of self-assembled multilayers are investigated as a function of number of deposited layers and dipping time on PEM cell performance. For comparison, the cell performance of original Nafion®117 based MEA with a loading of the same amount of catalyst (0.5 mg_{pt} cm^{-2}) is measured.

EXPERIMENTAL

Chemicals

Poly (allylamine hydrochloride) (PAH) (Mw: 15,000) was supplied from Aldrich and used as received. sPAni was synthesized according to Ito's report.[48] For this purpose, aniline (Ani), and ammonium peroxydisulfate (APS) were purchased from Aldrich and used without further purification. Hydrogen hexachloroplatinate (H_2PtCl_6) and sodium salts of borohydride were also obtained from Aldrich. Hispec 3000 (platinum, nominally 20% on carbon black) from E-TEK Company was used as catalyst. Vulcan XCR 72 (Cabot, bulk density of 6 Ibs ft^{-3}) was used as a catalyst support material. Commercial gas diffusion electrodes loaded 0.5 mg_{Pt} cm^{-2} were purchased from E-TEK Company. Nafion®117 commercial membrane was received from Ion Power Company (175 μm) with a nominal equivalent weight of 1100 g eq^{-1} while Nafion®117 solution (5%) was purchased from Quintech. Ultrapure hydrogen and air were supplied from commercial suppliers. Sulfuric acid (95–98%) and hydrogen peroxide (35%) were obtained from Riedel de Haen and used as received. In all lbl deposition experiments, Milli-Q ultrapure water (Millipore 18.2 MΩ at 25°C) was used. Prior to deposition, original Nafion membrane was treated according to our previous study to remove organic impurities and activate it.[49]

Techniques

Formation and thickness of self-assembled PAH/sPAni multilayers on the membrane support were observed using field emission scanning electron microscopy (FESEM). For SEM analysis, the sample broken after cooling in liquid nitrogen was sputtered with gold and measured by a FEI instrument at an operation voltage of 5 kV. Growth of the lbl multilayers consisting of PAH/sPAni was monitored using Perkin Elmer Lambda 35 series UV–vis spectroscopy with integrating sphere as a function of the number of deposited layers. Multilayer deposition of polyelectrolytes was automatically controlled by KSV dipping machine with a moving rate of 50 mm min^{-1}. Thermogravimetric analyses (TGA) of the self-assembled composite membranes were performed using TG/DTA 6300 SII Exstar with a heating rate of 10°C min^{-1} under nitrogen atmosphere from 40 to 700°C. Inductive coupling plasma-mass spectroscopy (ICP-MS) analysis was performed to determine catalyst loading inside lbl multilayers using Thermo Elemental X-series ICP-MS. Proton conductivities (σ) of the lbl self-assembled composite membrane and original Nafion were measured by two-probe method in water at 22 ± 1°C using a Solartron 1260 Frequency Response Analyzer (FRA) and Solartron 1296 Dielectric Interface (DI). The conductivity test system was described in a former publication.[50] To determine the electrical conductivity of powdered sPAni, both surfaces of sPAni pellets were coated with conductive liquid silver paint with a diameter of 10–15 mm and the measurements were performed using Novo Control Alpha-A Broad Band Dielectric Spectrometer. Prior conductivity

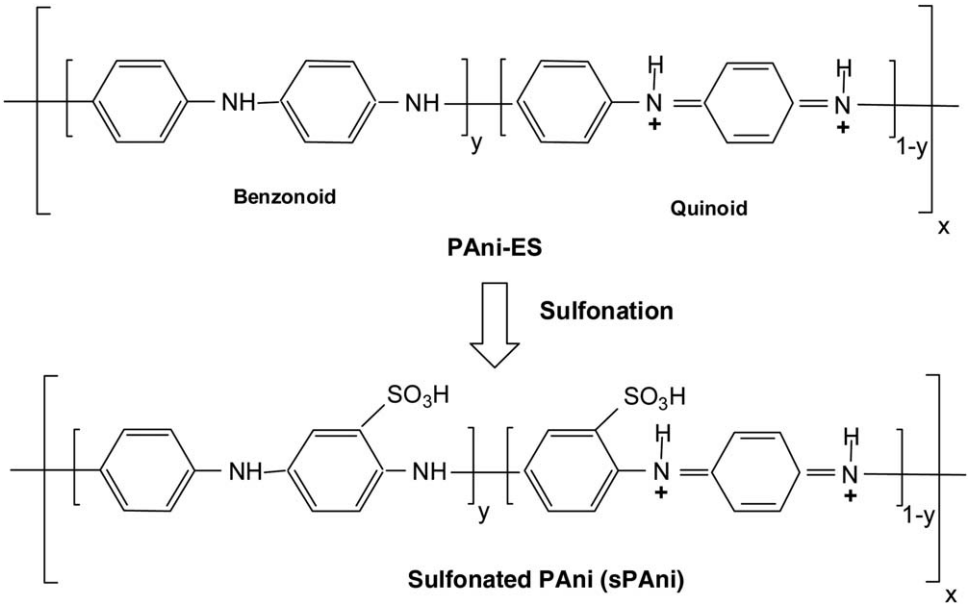

Scheme 1. Chemical structures PANi-ES and sPAni.

measurements of sPAni pellets, they were heated up to 100°C under nitrogen flow and waited for 2 h to eliminate humidity effects.

Preparation of PAni-ES

PAni in emeraldine salt form (PAni-ES) was prepared by chemical method as described in the literature.[51,52] For this purpose, freshly distilled Ani (0.02 mol) and 50 mL of 1 *M* HCl were placed into a three-necked round-bottomed flask. The mixture was then strongly stirred for 30 min. Subsequently APS (0.02 mol) solution in 50 mL of 1 *M* HCl was added using dropping funnel over 2 h. During this time, temperature of the mixture was below 5°C and the mixture was then reacted for further 2 h. After that time, the dark green precipitates of PAni-ES were washed four times with 100 mL of 1 *M* HCl and four times with 100 mL of acetone to remove impurities, such as unreacted monomer and APS. After the washing step, dark green PAni-ES was collected and dried in a vacuum oven at 60°C for 4 h. The chemical structure of PAni-ES is shown in Scheme 1.

Preparation of Sulfonated PAni

Sulfonation of PAni-ES was performed as reported in the literature.[48] PAni-ES (0.5 g) was firstly dispersed in 15.5 mL of 1,2-dichloroethane (DCE) and the mixture was heated to 80°C under reflux. The chlorosulfonic acid (1.25 g) was diluted with 1 mL of DCE by adding dropwise into the dispersion during 30 min and the reaction mixture was then held at 80°C for 5 h. Later sPAni was separated by filtration, immersed in 20 mL of water, and heated for 4 h at 100°C to promote its hydrolysis. Subsequently, sPAni was precipitated, washed by acetone, and it was finally dried in a vacuum oven at 60°C for 4 h. The chemical structure of sPAni is shown in Scheme 1.

Preparation of lbl Self-Assembled Composite Membrane

First, the solutions of PAH and sPAni in a concentration of 0.01 mol L^{-1} (mole for repeating unit) were prepared in Milli-Q water. pH of the PAH and sPAni solutions were adjusted to 1.8 and 2.5 by adding aqueous HCl, respectively, to achieve a relatively high charge density along the backbone and maintain the doped form of the sPAni. Multilayer formation started with the immersion of a negatively charged substrate (sulfonic acid groups of Nafion) into aqueous solution of cationic polyelectrolyte (PAH) so that a thin layer of this compound was adsorbed and the surface charge of the substrate reverted. Subsequent dipping of this substrate into a solution of anionic electrolyte (sPAni) again caused to adsorption of a thin layer and the surface charge was rendered negative again. Multiple repetitions of the adsorption steps yielded to a multilayer film with alternating positive and negative excess charges. To observe the effect of acid doping on fuel cell performance, some samples were immersed into 1 *M* of HCl for 1 h to obtain acid doped lbl composite membranes. The acid doped and undoped composite membranes were abbreviated as $(PAH/sPAni\text{-}H^{+})_n$ and $(PAH/sPAni)_n$, respectively where n is the number of deposited layers.

Preparation of lbl Catalyst Containing Membranes

In the preparation of CCMs, our modified method was applied to dope platinum (Pt) into lbl film.[46] In this method, 10 m*M* H_2PtCl_6 was first mixed with Vulcan and this mixture was subsequently dispersed into sPAni solution in the presence of Nafion (5 wt %) using an ultrasonic stirrer. Pretreated Nafion was then coated by alternately immersion of cationic (PAH) and platinum salt-Nafion and Vulcan containing anionic dipping solution (sPAni) as explained in "Preparation of lbl Self-Assembled Composite Membrane". Subsequently $PtCl_6^{-2}$ within the multilayers was reduced to platinum black clusters by soaking the composite membrane into 2 mM $NaBH_4$ solution for 30 min. Catalyst containing membranes are abbreviated as $(PAH/sPAni)_{n\text{-}Pt}$ where *n* is the number of deposited layers and Pt is the platinum.

MEA Preparation and Cell Performance Tests

For the preparation of 4 × 4 cm^2 MEAs based on lbl composite membrane or CCMs, 2.5 × 2.5 cm^2 commercial gas diffusion

Table I. Elemental Analysis and Conductivity Results for sPAni Samples

Products	Elemental analysis results					Conductivity at 25°C (S cm^{-1})
	C (%)	H (%)	N (%)	S (%)	S/N[a] ratio	
sPAni-1	33.19	4.14	6.9	15.74	1	0.4
sPAni-2	39.70	4.05	7.70	15.04	0.85	0.3

[a] In terms of moles of the S/N ratio at elemental analysis result.

electrodes (GDE) were assembled by hot pressing at 145°C and 250 psi for 5 min. Nafion spraying was also applied on the both sides of commercial GDEs to provide an improvement in electrode–electrolyte interaction.

Subsequently MEA was compressed between two bipolar plates (BPPs) using automatic fuel cell test fixture system under 5 bar. Concerning the cell performance test, 100 mL min^{-1} hydrogen and 300 mL min^{-1} dry air were fed into anode and cathode side, respectively. As it is known from the literature, the best performance values were obtained when MEA was performed under 100% humid environment.[53–57] That is why, the cell temperature was set to 75°C and the lines between humidification tanks and cell were heated up higher temperature than 75°C to prevent possible water condensation. Upon the performance test, the heater, and humidification lines were purged with nitrogen and MEAs were conditioned for 6 h under reactant and oxidant feeding at 100% humidified condition and 75°C. The polarization curves were finally obtained by scanning at a rate of 2.5 mVs^{-1} from open circuit voltage (OCV) to 0.1 V and the tests were repeated several times to obtain accurate cell performance results.

RESULTS AND DISCUSSION

Water solubility and parallel ionic/electronic conductivity of sPAni prompted us to construct two different nanostructured membrane electrode assemblies (MEA) based on lbl composite and Pt containing membrane. It was expected that sPAni's ability to electron and proton conductivity may make it possible to provide better triple-phase contact and to achieve higher cell performance. Furthermore, Nafion membranes in different thickness as support material for H_2/O_2 cells were used in order to investigate the effect of electrolyte thickness on cell performance.

Synthesis and Characterization of sPAni

PAni-ES was synthesized via precipitation polymerization by mixing an aqueous solution of Ani and an oxidant. Afterward, water-soluble acid doped sPAni was prepared by the following synthetic technique in which PAni-ES was sulfonated by chlorosulfonic acid in dichloroethane at 80°C and subsequently hydrated in water at 100°C as reported in the literature.[48] Since it was found that the dissolution of sPAni in water mainly depended on the level of sulfonation degree, water solubility of the sulfonated product was examined as a function of the degree of sulfonation (DS), namely sulfur-to-nitrogen (S/N) ratio, by adjusting the amount of chlorosulfonic acid. Elemental analysis of the synthesized sPAni was performed to determine sulfonation degree from S/N ratio. Elemental analysis results for two different sulfonated products synthesized in the same way are presented in Table I.

Although the S/N ratio for sPAni was reported as 0.8 in the literature, S/N ratios of sPAni samples prepared here by following the same method were found to be 0.85 and 1. In correlation with the previously reported result by Ito et al.[48] the water solubility of the synthesized sPAni (S/N: 0.85) was found to be more than 50 g L^{-1}. Furthermore the electrical conductivities of sPAni powdered samples were found to be 0.3 and 0.4 S cm^{-1} for sPAni samples with S/N ratios of 0.85 and 1, respectively. The obtained conductivity results were in good agreement with the literature.[26]

Besides, TG analysis of PAni-ES and sPAni were performed to investigate the sulfonation effect on thermal stability and thermal degradation curves are given in Figure 1. PAni-ES lost its weight of 10% until 180°C due to the adsorbed water. This was followed by decomposition of PAni backbone starting from 340°C. In contrast to PAni-ES, one can clearly see from Figure 1 that the thermal degradation of sPAni took place at lower temperatures as compared to PAni-ES and it occured over two steps beginning from 170°C where the sulfonic acid group of sPAni begun to decompose. Subsequently, thermal degradation at around 335°C corresponded to the degradation of polymer backbone. On the other hand, the char residues for PAni-ES and sPAni were found to be 52 and 35% at 800°C under inert atmosphere, respectively.

Characterization of lbl Composite Membranes

UV–vis Measurements. UV–visible spectroscopy was used to monitor the growth of the self-assembled multilayers on Nafion

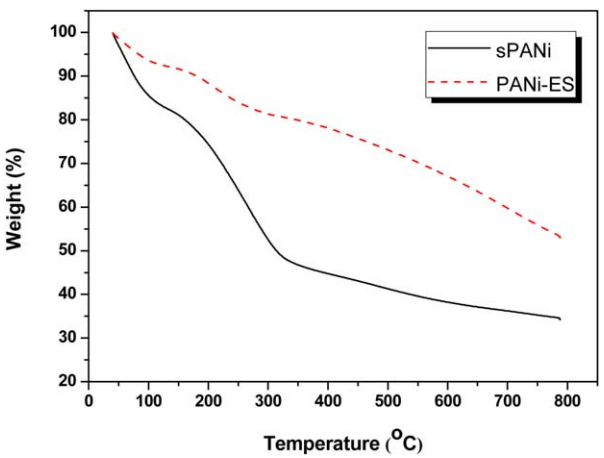

Figure 1. TGA curves of PANi-ES and sPAni. [Color figure can be viewed in the online issue, which is available at wileyonlinelibrary.com.]

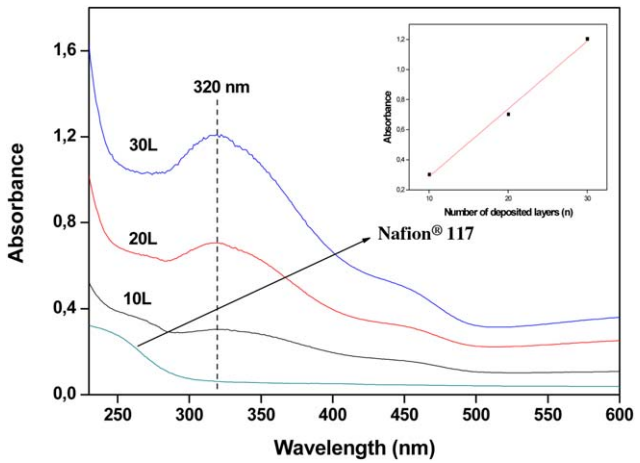

Figure 2. UV–vis absorption spectra of $(PAH/sPAni\text{-}H^{+})_n$ ($n = 10$–30). [Color figure can be viewed in the online issue, which is available at wileyonlinelibrary.com.]

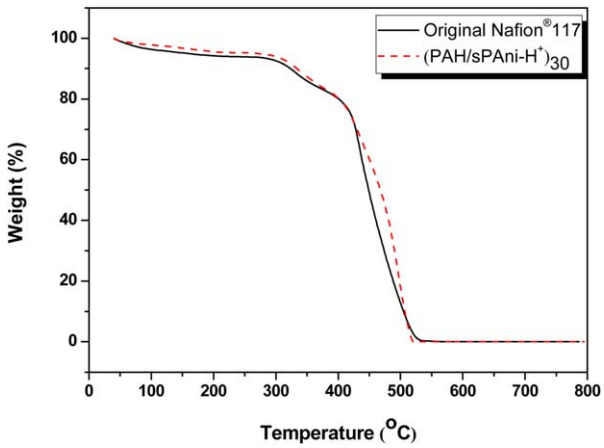

Figure 4. TGA curves of $(PAH/sPAni\text{-}H^{+})_{30}$ composite membrane and original Nafion®117. [Color figure can be viewed in the online issue, which is available at wileyonlinelibrary.com.]

surface. UV–visible spectra of the $(PAH/sPAni)_{10–30}$ on Nafion as a function of the number of adsorbed layers are shown in Figure 2.

Absorbance at 320 nm is related to the characteristics wavelength for HCl doped PAni (PAni-ES). This spectrum of PAni is assigned for the π–π^* transition at 320 nm. Since PAH is transparent in the UV–vis spectral range, the increase in the absorbance can be directly attributed to the adsorption of sPAni on Nafion surface. As it can be seen from UV–vis spectra, the absorbance increased with the number of deposited layers. This result showed that synthesized sPAni can be adsorbed on the surface regularly.

To see the effect of sPAni deposition, proton conductivities (σ) of lbl composite membrane $(PAH/sPAni\text{-}H^{+})_{30}$, and original Nafion®117 were determined. The Nyquist plots of the products are shown in Figure 3.

As one can see from the figure that the bulk resistance of acid doped lbl composite membrane $(PAH/sPAni\text{-}H^{+})_{30}$ was significantly lower than that of original Nafion®117. In other word, σ values of lbl composite membrane and original Nafion®117 were found to be 200 and 62.3 mS cm^{-1}, respectively. This significant improvement in σ can be explained as follows: chemical treatment of original Nafion®117 membrane with H_2O_2 and H_2SO_4 prior to lbl deposition leads to a sharp increase in conductivity (150.6 mS cm^{-1}). This result can be attributed to the opening and swelling of the pores after chemical treatment. A similar result was reported by Ramdutt et al. previously.[58] Also, a further increase in σ from 150.6 to 200 mS cm^{-1} can be corresponded to the acid doping of sPAni leading to formation of emaraldine salt form which has high electronic conductivity.

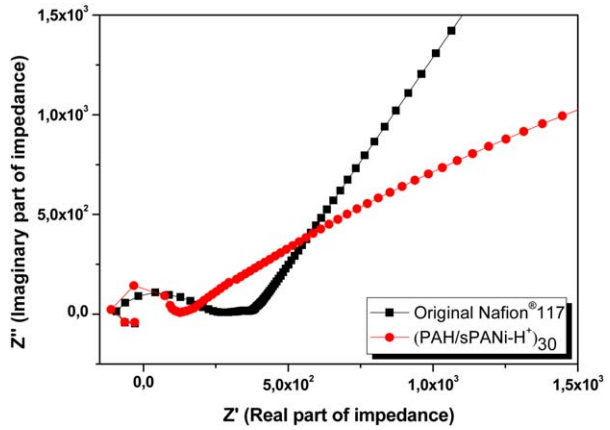

Figure 3. Nyquist plots of $(PAH/sPAni\text{-}H^{+})_{30}$ and original Nafion®117 membranes. [Color figure can be viewed in the online issue, which is available at wileyonlinelibrary.com.]

TG Analysis. TGA patterns of acid doped lbl composite membrane consisting of 30 bilayers of PAH/sPAni and pure Nafion®117 are shown in Figure 4.

As one can see from the figure, thermal decomposition of original Nafion®117 occurred in three steps. These steps can be attributed to water loss (i), decomposition of side chain group ($–SO_3H$) (ii), and degradation of polytetraflouroethylene (PTFE) backbone (iii), respectively. While the first weight loss occurred between 40 and 150°C, decomposition of sulfonic acid groups of Nafion started at 290°C. Finally, the polymer backbone degradation took place above 400°C. Similar thermal degradation curves were previously reported by Surowiec and Bogoczek for original Nafion®117 in proton form.[59] Concerning the thermal degradation behavior of lbl composite membrane, it can be seen from the figure that thermal degradation of composite membrane with a deposition of 30 layer of $PAH/sPAni\text{-}H^{+}$ (S/N ratio = 0.85) slightly enhanced as compared to the original Nafion membrane. This result is consistent with our previous result.[49] This increase in the thermal stability of lbl composite membrane can be attributed to the formation of polyelectrolyte complex between sulfonic acid group of Nafion and amine group of PAH. Conclusively, it can be emphasized from TGA curves that the thermal decomposition of lbl composite membrane does not take place until 290°C and it is highly suitable for H_2/O_2 fuel cell applications.

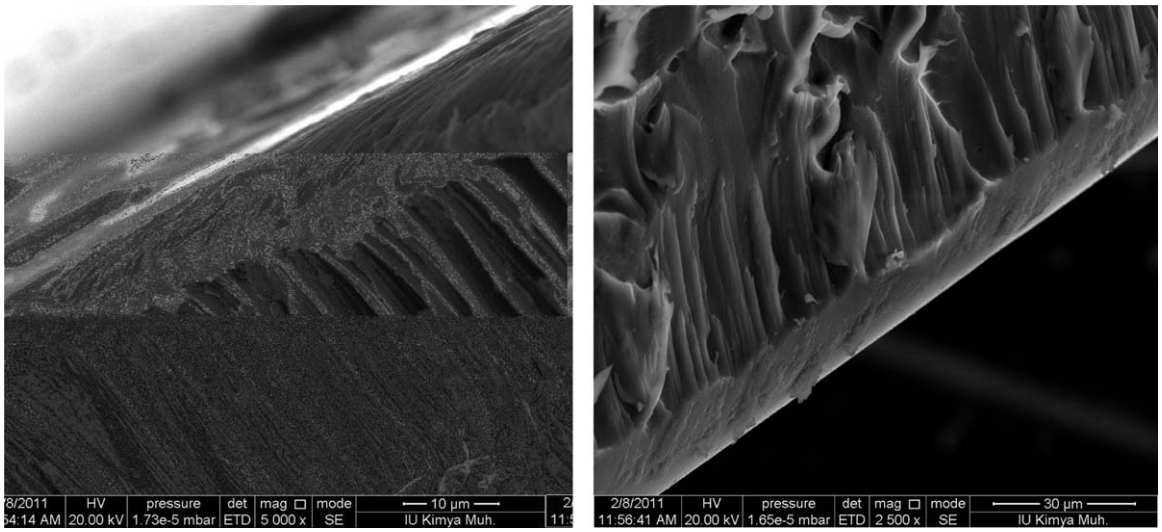

Figure 5. SEM picture of $(PAH/sPAni\text{-}H^{+})_{10}$ composite membrane.

SEM Analysis

SEM pictures of the lbl composite membrane prepared from 30 layers deposition of PAH/sPAni were taken to observe the multilayer formation. The pictures are shown in Figure 5. As it was seen from the figure, polyelectrolytes were deposited on both sides of the pretreated Nafion membrane homogenously as suggested by UV–vis analysis. The thickness of $(PAH/sPAni\text{-}H^{+})_{30}$ was found to be at the range of 5 μm. Comparing with the literature, it can be said that the thickness of one layer of lbl composite membrane obtained from PAH and sPAni was significantly higher than that of self-assembled membrane prepared from PAH and PSS reported in the literature.[23] In addition, the surface of the membrane was dense and smooth.

Single Cell Performances

lbl Composite Membrane Based MEAs. Single cell performances of lbl composite membrane based MEAs were measured to optimize the some important lbl deposition parameters, such as number of deposited layers, deposition time and acid doping. Figure 6 shows the polarization and power density curves of MEAs prepared by hot pressing of $(PAH/sPAni)_{10}$-C paper GDE and $(PAH/sPAni)_{30}$-C paper GDE under the pressing conditions as explained in "MEA Preparation and Cell Performance Tests".

From the figure, it can be observed that the maximum power outputs of 10 and 30 layers of lbl self-assembled composite membrane $(PAH/sPAni)_{10}$ and $(PAH/sPAni)_{30}$ based MEAs were 91 and 82 mW cm^{-2}, respectively. Thus, the reduction in the number of deposited layers led to a slight enhancement in single cell performance of MEA. This probably can be attributed to the low ohmic polarization losses through electrolyte due to the formation of thinner lbl multilayers with less number of deposition steps. Again, it can be seen from the figure that mass polarization loss was low if less number of multilayers were deposited on the surface.

To improve the single cell performance of $(PAH/sPAni)_n$ based MEAs, lbl composite membrane was doped by HCl as explained in "Preparation of lbl Self-Assembled Composite Membrane". The obtained single cell performance results are presented in Figure 7. It was found from the figure that the power density of MEA based on acid doped lbl self-assembly of 10 layers of PAH/sPAni composite membrane enhanced and it reached to 126 mW cm^{-2} (black rectangular in Figure 7). This improvement in cell performance from 91 to 126 mW cm^{-2} may be corresponded to increment in the charge density inside lbl multilayers and improvement in electronic conductivity of sPAni due to its self-conjugated structure upon acid doping. In that case, it is expected that more effective triple phase boundary (TPB) can be formed. On the other hand, we can also conclude that electrically conductive lbl multilayers prepared from PAH/sPAni enhanced PEMFC performance as compared to lbl composite multilayers obtained from the electrical nonconducting polyelectrolytes. For example, the cell performance of MEA based on 10 layers of lbl PAH/PSS (polystyrenesulfonic acid) composite membrane was found to be around 98 mW cm^{-2}[47]

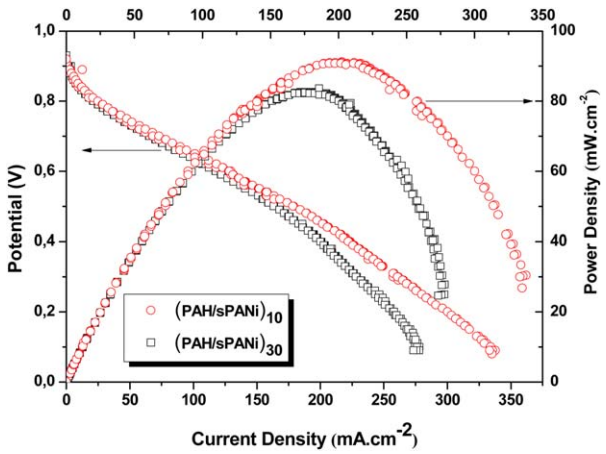

Figure 6. Polarization and power density curves of MEA prepared by pressing of $(PAH/sPAni)_{10}$ and $(PAH/sPAni)_{30}$ composite membrane and commercial C paper-based GDE. (Hydrogen flow rate: 100 mL min^{-1}, air flow rate: 300 mL min^{-1}, humidity: 100% and cell temperature: 75°C.) [Color figure can be viewed in the online issue, which is available at wileyonlinelibrary.com.]

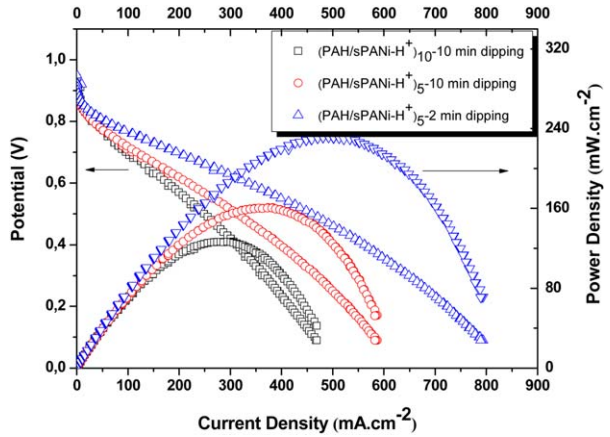

Figure 7. Polarization and power density curves of MEA based on acid doped $(PAH/sPAni\text{-}H^+)_{10}$ and $(PAH/sPAni\text{-}H^+)_5$ composite membrane with a different deposition time (10 and 2 min) and commercial C-paper-based GDE. (Hydrogen: 100 mL min^{-1}, air flow rate: 300 mL min^{-1}, humidity: 100%, and cell temperature: 75°C.) [Color figure can be viewed in the online issue, which is available at wileyonlinelibrary.com.]

while the analog MEA, $(PAH/sPAni\text{-}H^+)_{10}$, showed a maximum power output of 126 mW cm^{-2}.

In a series of experiments, it was aimed to prepare acid doped lbl composite membrane with less number of deposited layers. Figure 7 also shows that the cell performance of MEA prepared from acid doped five layers of PAH/sPAni lbl self-assembled composite membrane, $(PAH/sPAni)_5\text{-}H^+$. In this case, the maximum power output rose from 126 to 160 mW cm^{-2} with 50% reduction in the number of deposited layers. This significant improvement in power density can be mainly explained by facilitated proton transfer through electrolyte leading to lower ohmic resistance. Besides H_2/O_2 cell performance of MEA obtained from five layers self-assembly of PAH/sPAni with a deposition time of 2 min was tested and it was found that the maximum power output of this MEA was significantly higher (231 mW cm^{-2}) than that of MEA based on original Nafion®117 (198 mW cm^{-2}). This result showed the strong effect of number of deposited layers or in other word, multilayer thickness on PEM cell performance. Importantly, this obtained result prompted us to apply thinner lbl multilayers by controlling (i) the number of deposited layers and (ii) dipping time for achieving higher cell performance.

Catalyst Containing Membrane (CCM) Based MEAs. As it was reported in the literature,[47] interfacial areas between the reactant, electrolyte and catalyst, called the triple phase boundary (TPB), play an important role for the performance of PEMFCs. To effectively utilize the catalyst, the TBP which is located in MEA, has to find a balance between the ionic and electronic conducting media, allowing continuous pathways of the protons to the electrolyte and electrons to the electrode. For this purpose, it was developed a series nanostructured MEAs based on lbl self-assembled CCMs for achieving high H_2/O_2 fuel cell activity. Also, it was targeted to prepare thinner MEAs for further improvement in power density. Pt loaded MEAs were prepared from 10 layers self-assembly of PAH and platinum catalyst containing sPAni using lbl technique as explained in "Preparation of lbl Catalyst Containing Membranes".

Figure 8 illustrates the polarization and power density curves of Pt containing lbl membrane based MEAs. As one can see from the figure, the peak power density of MEA obtained from 10 multilayers of PAH and sPAni containing platinum salt-Nafion and Vulcan $(PAH/sPAni)_{10\text{-}Pt}$ was found to be 113 mW cm^{-2}. This result shows that Pt containing membrane based MEA has roughly 20% higher maximum power density than that of corresponding lbl composite membrane $(PAH/sPAni)_{10}$ based MEA (see Figure 6, maximum peak power density: 91 mW cm^{-2}). This increase can be explained by the formation of more effective TPB in the presence of extra catalyst inside lbl multilayers if catalyst containing membrane-electrode was employed. However, this Pt containing membrane based MEA had significantly lower power peak density than that of MEA obtained from original Nafion®117 (198 mW cm^{-2}). One can see from Figure 8 that $(PAH/sPAni)_{10\text{-}Pt}$ based MEA has highest activation and ohmic resistance among other MEAs. This result can be attributed to the formation of thick adsorbed layers including metallic Pt on the each side of Nafion membrane blocking both proton passages along the electrolyte and the transport of hydrogen onto catalytic active sites. On the other hand, ICP-MS analysis of platinum containing lbl membrane was performed to determine the amount of catalyst trapped inside lbl multilayer and it was found to be 0.32 μg cm^{-2}. This low platinum deposition within lbl multilayers can be considered as understandable due to the total thickness of deposited layers.

To show the critical effect of electrolyte thickness on cell activity, a thin electrolyte in 30 μm thickness was prepared using Nafion®117 solution via spraying and then the procedure reported in "Preparation of lbl Catalyst Containing Membranes" was followed for the preparation of nanostructured MEA from catalyst containing lbl self-assembled membrane. Promisingly, the cell performance of this MEA was significantly improved (81.8%) and reached to 360 mW cm^{-2} as compared to MEA

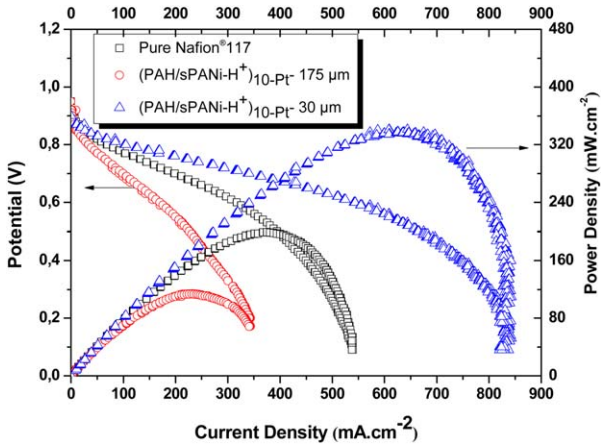

Figure 8. Polarization and power density curves of MEA based on PAH/sPAni lbl CCMs and original Nafion®117 (Hydrogen flow rate: 100 mL min^{-1}, air flow rate: 300 mL min^{-1}, humidity: 100%, and cell temperature: 75°C.) [Color figure can be viewed in the online issue, which is available at wileyonlinelibrary.com.]

based on original Nafion®117. We believe that the main reason for this sharp increase in cell performance was due to the use of thin electrolyte than commercial proton conducting membranes (around 175 μm). It was also found from Figure 8 that thinner electrolyte caused a dramatic reduction in ohmic resistivity along the electrolyte as well as lowered activation polarization losses. The other reason for the observed highest peak power performance of thin Pt containing membrane based MEA is sPAni's ability to simultaneous electron and proton conductivity. This property of sPAni can cause a more effective TPB region in lbl self-assembled electrocatalyst layer. On the other hand, the mass transport polarization of MEA prepared from catalyst containing membrane, $(PAH/sPAni)_{10\text{-}Pt}$, was found to be slightly higher than that of original Nafion®117 based MEA. This behavior can be attributed to the formation of Pt including multilayers which may restrict the diffusion of gas or products at the cathode side. Furthermore, Pt utilization of the $(PAH/sPAni\text{-}H^+)_{10\text{-}Pt}$ based MEA was found to be 720 mW $mgPt^{-1}$ which was very comparable to the literature.[24,44,46] As it is known, Pt utilization is related to TPB and mainly responsible for the performance of a PEMFC.[57] We believe that the optimization of these interfaces can be possible by fine tuning the electrode–electrolyte structure at the nano scale level using lbl technique. In conclusion, we can claim that the construction of thin and highly conductive platinum containing lbl membranes is very suitable for achieving higher H_2/O_2 fuel cell activity and further enhancement in single cell performance can be maintained by acid doping. Similarly, we can offer platinum containing lbl membranes for direct methanol fuel cells (DMFC).

CONCLUSION

In this study, two different types of MEA constructions based on layer-by-layer (lbl) composite and catalyst containing membrane (CCM) from polyallylamine hydrochloride (PAH) and sulfonated polyaniline (sPAni) are described. Furthermore, H_2/O_2 fuel cell performances of these MEAs are compared. SEM and UV–vis analysis show that the multilayers are deposited on both sides of Nafion support successfully. The single cell performances of MEAs prepared from acid doped 5 and 10 layers of lbl self-assembled composite membrane, $(PAH/sPAni\text{-}H^+)_5$ and $(PAH/sPAni\text{-}H^+)_{10}$, display the power output of 160 and 126 mW cm^{-2}, respectively. This result can be mainly attributed to the facilitated proton transfer through electrolyte leading to lower ohmic resistance if less number of multilayers is coated. In addition, H_2/O_2 cell performance of MEA prepared from five layers of self-assembly of PAH/sPAni with a deposition time of 2 min is found to be 231 mW cm^{-2} which is significantly higher than that of MEA based on original Nafion®117 membrane (198 mW cm^{-2}). This result shows the strong effect of number of deposited layers on single cell activity.

For comparison, H_2/O_2 fuel cell peak power density of MEA obtained from catalyst containing membrane $(PAH/sPAni)_{10\text{-}Pt}$, is tested and it is found to be 113 mW cm^{-2} which is roughly 20% higher than that of corresponding lbl composite membrane based MEA. This is probably due to increased probability of the triple phase contact in the presence of extra platinum within lbl multilayers. Moreover, MEA obtained from thinner (30 μm) catalyst containing membrane $(PAH/sPAni)_{10\text{-}Pt}$, exhibits a peak power output of 360 mW cm^{-2} with a Pt utilization of 720 mW $mgPt^{-1}$. This performance is 81.8% higher as compared to original Nafion®117 based MEA. From the analyses of the cell performance evaluations for different structured MEAs, two main conclusions can be drawn:

- A high activity MEA for H_2/O_2 fuel cells can be fabricated from catalyst containing membranes and use of thin electrolyte favors the cell performance.
- The use of sPAni can lead to more effective triple phase boundary (TPB) since its ability to simultaneous electron and proton conductivity at the electrocatalyst layer. The other advantage for deposition of sPAni is leading to superior physicochemical properties such as conductivity and thermal stability.

ACKNOWLEDGMENTS

This study was supported by TUBITAK, under the contract number of 109M546.

REFERENCES

1. Mehta, V.; Cooper, J. S. *J. Power Sources* **2003**, *114*, 32.
2. Frey, T.; Linardi, M. *Electrochim. Acta* **2004**, *50*, 99.
3. Zhang, Y. J.; Wang, C.; Wan, N. F.; Liu, Z. X.; Mao, Z. Q. *Electrochem. Commun.* **2007**, *9*, 667.
4. Prasanna, M.; Ha, H. Y.; Cho, E. A.; Hong, S.-A.; Oh, I.-H. *J. Power Sources* **2004**, *137*, 1.
5. Hu, M.; Sui, S.; Zhu, X.; Yu, Q.; Cao, G.; Hong, X.; Tu, H. *Int. J. Hydrogen Energy* **2006**, *31*, 1010.
6. Sun, L.; Ran, R.; Shao, Z. *Int. J. Hydrogen Energy* **2010**, *35*, 2921.
7. Cheng, X.; Yi, B.; Han, M.; Zhang, J.; Qiao, Y.; Yu, J. *J. Power Sources*, **1999**, *79*, 75.
8. Sun, L. L.; Ran, R.; Wang, G. X.; Shao, Z. P. *Solid State Ionics* **2008**, *179*, 21.
9. Wang, D.; Wang, L.; Liang, J.; Xia, Z.; Wang, S.; Zhu, Y.; Liu, C.; Sun, G. *J. Power Sources* **2013**, *224*, 202.
10. Su, H.; Liao, S.; Shu, T.; Gao, H. *J. Power Sources* **2010**, *195*, 756.
11. Vengatesan, S.; Kim, H.-J.; Lee, S.-Y.; Cho, E.; Ha, H. Y.; Oh, I.-H.; Lim, T.-H. *J Power Sources* **2007**, *167*, 325.
12. Cindrella, L.; Kanan, A. M. *J. Power Sources* **2009**, *193*, 447.
13. Leimin, X.; Shijun, L.; Lijun, Y.; Zhenxing, L. *Fuel Cells* **2009**, *9*, 101.
14. Thanasilp, S.; Hunsom, M. *Fuel* **2010**, *89*, 3847.
15. Kim, K. H.; Lee, K-Y.; Lee, S-Y.; Cho, E.; Lim, T. H.; Kim, H. J.; Yoon, S. P.; Kim, S. H.; Lim, T. W.; Jang, J. H. *Int. J. Hydrogen Energy* **2010**, *35*, 13104.
16. Xiong, L.; Manthiram, A. *Electrochim. Acta* **2005**, *50*, 3200.
17. Tang, H. L.; Wang, S. L.; Pan, M.; Jiang, S. P. *Electrochim. Acta* **2007**, *52*, 3714.
18. Saha, M. S.; Paul, D. K.; Peppley, B. A.; Karan, K. *Electochem. Commun.* **2011**, *12*, 410.

19. Roy, A.; Hickner, M. A.; Lane, O.; McGrath, J. E. *J. Power Sources* **2009**, *191*, 550.
20. Suzuki, T.; Tabuchi, Y.; Tsushima, S.; Hirai, S. *Int. J. Hydrogen Energy* **2011**, *36*, 5479.
21. Kim, C. S.; Chun, Y. G.; Peck, D. H.; Shin, D. R. *Int. J. Hydrogen Energy* **1998**, *23*, 1045.
22. Towne, S.; Viswanathan, V.; Holbery, J.; Rieke, P. *J. Power Sources* **2007**, *171*, 575.
23. Decher, G. *Science* **1997**, *277*, 1232.
24. Michel, M.; Taylor, A.; Sekol, R.; Podsiadlo, P.; Ho, P.; Kotov, N.; Thompson, L. *Adv. Mater.* **2007**, *19*, 3859.
25. Ho, K. S.; Hsieh, K. H.; Huang, S. K.; Hsieh, T. H. *Synth. Met.* **1999**, *10*, 65.
26. Stejskal, J.; Gilbert, R. G. *Pure Appl. Chem.* **2002**, *74*, 857.
27. Haba, Y.; Sagal, E.; Narkis, M.; Titelman, G. I.; Siegmann, A. *Synth. Met.* **2000**, *110*, 189.
28. Kinlen, P. J.; Liu, J.; Ding, Y.; Graham, C. R.; Remsen, E. E. *Macromolecules* **1998**, *31*, 1735.
29. Sotomura, T.; Uemachi, H.; Takeyama K.; Naoi, K.; Oyama, N. *J. Electrochem. Soc.* **1995**, *142*, L47.
30. Yang, Y.; Westerweele, E.; Zhang, C.; Smith, P.; Heeger, A. J. *J. Appl. Phys.* **1995**, *77*, 694.
31. Barnes, A.; Despotakis, A.; Wong, T. C. P.; Anderson, A. P.; Chambers, B.; Wright, P. V. *Mater. Struct.* **1998**, *7*, 752.
32. Jiang, Y.; Epstein, A. J. *J Am. Chem. Soc.* **1990**, *112*, 2880.
33. Yue, J.; Wang, Z. H.; Cromack, K. R.; Epstein, A. J.; MacDiarmid, A. G. *J. Am. Chem. Soc.* **1991**, *113*, 2665.
34. Deligöz, H.; Yılmaztürk, S.; Karaca,T.; Özdemir, H.; Öksüzömer, F.; Koç, S. N.; Durmuş, A.; Gürkaynak, M. A. *J. Membr. Sci.* **2009**, *326*, 643.
35. Kim, D. W.; Choi, H. C.; Lee, B. G.;Blumstein, A.; Kang, Y. *Electrochim. Acta* **2004**, *50*, 659.
36. Ok, J.; Kim, D. W.; Lee, C.; Choi, W. C.; Cho, S.; Kang, Y. *Bull. Korean Chem. Soc.* **2008**, *29*, 842.
37. Jiang, S. P.; Liu, Z.; Tian, Z. Q. *Adv. Mater.* **2006**, *18*, 1068.
38. Argun, A. A.; Ashcraft, J. N.; Hammond, P. T. *Adv. Mater.* **2008**, *20*, 1539.
39. Zhao, C.; Lin, H.; Zhang, Q.; Na, H. *Int. J. Hydrogen Energy* **2010**, *35*, 10482.
40. Antolini, E.; Gonzalez, E. R. *Appl. Catal. A* **2009**, *365*, 1.
41. Farhat, T. R.; Hammond, P. T. *Adv. Funct. Mater.* **2005**, *15*, 945.
42. Farhat, T. R.; Hammond, P. T. *Adv. Funct. Mater.* **2006**, *16*, 433.
43. Farhat, T. R.; Hammond, P. T. *Chem. Mater.* **2006**, *18*, 41.
44. Taylor, A. D.; Michel, M.; Sekol, R. C.; Kizuka, J. M.; Kotov, N. A.; Thompson, L. *Adv. Funct. Mater.* **2008**, *18*, 3003.
45. Yuan, J.; Wang, Z.; Zhang, Y.; Shen, Y.; Han, D.; Zhang, Q.; Xu, X.; Niu, L. *Thin Solid Films* **2008**, *516*, 6531.
46. Yılmaztürk, S.; Gümüşoğlu, T.; Arı, G.; Öksüzömer, F.; Deligöz, H. *J. Power Sources* **2012**, *201*, 88.
47. Michel, M.; Ettingshausen, F.; Scheiba, F.; Wolz, A.; Roth, C. *Phys. Chem. Chem. Phys.* **2008**, *10*, 3796.
48. Ito, S.; Murata, K.; Teshima, S.; Aizawa, R.; Asako, Y.; Takahashi, K.; Hoffman, B. M. *Synth. Met.* **1998**, *96*, 161.
49. Yılmaztürk, S.; Deligöz, H.; Yılmazoğlu, M.; Damyan, H.; Öksüzömer, F.; Koç, S. N.; Durmuş, A.; Gürkaynak, M. A. *J. Power Sources* **2010**, *195*, 703.
50. Deligöz, H.; Yılmazturk, S.; Karaca, T.; Özdemir, H.; Koç, S. N.; Öksüzömer, F.; Durmuş, A.; Gürkaynak, M. A. *J. Membr. Sci.* **2009**, *326*, 643.
51. Deligöz, H.; Tieke B. *Macromol. Mater. Eng.* **2006**, *291*, 793.
52. Deligöz H. *J. Appl. Polym. Sci.* **2007**, *105*, 2640.
53. Zhang, J.; Tang, Y.; Song, C.; Cheng, X.; Zhang, J.; Wang, H. *Electrochim. Acta* **2007**, *52*, 5095.
54. Xu, H.; Kunz, H. R.; Fenton, J. M. *Electrochim. Acta* **2007**, *52*, 3525.
55. Guvelioglu, G. H.; Stenger, H. G. *J. Power Sources* **2007**, *163*, 881.
56. Zhang, J.; Tang, Y.; Song, C.; Xia, Z.; Li, H.; Wang, H.; Zhang J. *Electrochim. Acta* **2008**, *53*, 5315.
57. O'Hayre, R.; Barnett, D. R.; Prinz, F. F. *J. Electrochem. Soc.* **2005**, *152*, A439.
58. Ramdutt, D.; Charles, C.; Hudspeth, J.; Ludewig, B.; Gagenbach, T.; Boswell, R.; Dicks, A.; Brault, P. *J. Power Sources*, **2007**, *165*, 41.
59. Surowiec, J.; Bogoczek, R. *J. Therm. Anal.* **1988**, *33*, 1097.